RESEARCH   **Open Access**

Neuroinflammation is associated with Alzheimer's disease co-pathology in dementia with Lewy bodies

Janna van Wetering[1,2] , Hanne Geut[1,2], John J. Bol[1], Yvon Galis[1], Evelien Timmermans[1], Jos W.R. Twisk[3], Dagmar H. Hepp[4], Martino L. Morella[1,2], Lasse Pihlstrom[5], Afina W. Lemstra[2,6,7], Annemieke J.M. Rozemuller[2,8], Laura E. Jonkman[1,2] and Wilma D.J. van de Berg[1,2]*

Abstract

Background Neuroinflammation and Alzheimer's disease (AD) co-pathology may contribute to disease progression and severity in dementia with Lewy bodies (DLB). This study aims to clarify whether a different pattern of neuroinflammation, such as alteration in microglial and astroglial morphology and distribution, is present in DLB cases with and without AD co-pathology.

Methods The morphology and load (% area of immunopositivity) of total (Iba1) and reactive microglia (CD68 and HLA-DR), reactive astrocytes (GFAP) and proteinopathies of alpha-synuclein (KM51/pser129), amyloid-beta (6 F/3D) and p-tau (AT8) were assessed in a cohort of mixed DLB + AD ($n=35$), pure DLB ($n=15$), pure AD ($n=16$) and control ($n=11$) donors in limbic and neocortical brain regions using immunostaining, quantitative image analysis and confocal microscopy. Regional and group differences were estimated using a linear mixed model analysis.

Results Morphologically, reactive and amoeboid microglia were common in mixed DLB + AD, while homeostatic microglia with a small soma and thin processes were observed in pure DLB cases. A higher density of swollen astrocytes was observed in pure AD cases, but not in mixed DLB + AD or pure DLB cases. Mixed DLB + AD had higher CD68-loads in the amygdala and parahippocampal gyrus than pure DLB cases, but did not differ in astrocytic loads. Pure AD showed higher Iba1-loads in the CA1 and CA2, higher CD68-loads in the CA2 and subiculum, and a higher astrocytic load in the CA1-4 and subiculum than mixed DLB + AD cases. In mixed DLB + AD cases, microglial load associated strongly with amyloid-beta (Iba1, CD68 and HLA-DR), and p-tau (CD68 and HLA-DR), and minimally with alpha-synuclein load (CD68). In addition, the highest microglial activity was found in the amygdala and CA2, and astroglial load in the CA4. Confocal microscopy demonstrated co-localization of large amoeboid microglia with neuritic and classic-cored plaques of amyloid-beta and p-tau in mixed DLB + AD cases.

Conclusions In conclusion, microglial activation in DLB was largely associated with AD co-pathology, while astrocytic response in DLB was not. In addition, microglial activity was high in limbic regions, with prevalent

*Correspondence:
Wilma D.J. van de Berg
wdj.vandeberg@amsterdamumc.nl

Full list of author information is available at the end of the article

AD pathology. Our study provides novel insights into the molecular neuropathology of DLB, highlighting the importance of microglial activation in mixed DLB + AD.

Keywords Lewy body disease, Dementia with Lewy bodies, Alzheimer's disease, Co-pathology, Neuroinflammation, Alpha-synuclein, Amyloid-beta, Phosphorylated-tau, Microglia, Astroglia, Post-mortem, Immunohistochemistry

Background

The incidence of dementia is increasing rapidly as the population ages [1, 2]. Alzheimer disease (AD) and dementia with Lewy bodies (DLB) are the two most common subtypes of neurodegenerative dementia [3]. While AD and DLB have overlapping clinical features, AD is characterized by impairment in memory and learning, executive function and aphasia, whilst the core clinical features of DLB include visual hallucinations, cognitive fluctuations, rapid eye movement (REM) sleep behavior disorder (RBD) and parkinsonism [3, 4]. The clinical presentation of DLB can vary widely between patients in terms of disease onset, disease progression, treatment response and adverse side effects.

Protein misfolding, accumulation and aggregation are the primary pathological hallmarks of both DLB and AD [4]. In DLB, abnormal alpha-synuclein (α-syn) accumulates and aggregates in neurons, leading to the formation of Lewy bodies (LBs) and Lewy neurites (LNs), which are typically found in the brainstem, limbic and neocortical areas, spinal cord and peripheral nervous system [5]. AD is characterized by the deposition of extracellular amyloid beta (Aβ) plaques and intracellular phosphorylated tau (p-tau) tangles [6, 7]. Approximately 50–80% of DLB cases exhibit AD co-pathology, while circa 50% of AD cases show α-syn pathology in the amygdala and other limbic regions, as observed in clinicopathological studies [8–10]. On top of that, within Lewy body disorders (LBD), the amygdala is suggested to be prone to even initiate the development of α-syn pathology [11] and function as an incubator for coexisting pathologies such as Aβ and p-tau [12]. Accumulating evidence from disease models reports interactions between α-syn, p-tau and Aβ pathology, which together form a destructive feedforward loop towards more severe and faster neurodegeneration [13–16]. Compared to separate pathology, the combination of α-syn, p-tau, and Aβ semi-quantitative pathology scores best predict cognitive decline, as measured by the MMSE [17]. In addition, DLB patients with AD co-pathology show a highly aggressive disease course with rapid cognitive decline compared to pure DLB cases [4, 18–20]. More importantly, aggregation of α-syn, p-tau, and Aβ pathology is associated with the activation of innate and adaptive immune responses in the elderly [21].

It is well established that, in AD, the innate immune system is activated in early stages of the disease, and reactive microglia and astrocytes surrounding Aβ plaques are frequently described [22–25]. Regional differences in glial activation have been reported in PD and DLB cases compared to controls, with some studies suggesting a higher activated microglial load, as measured by HLA-DR or CD68, in the amygdala [26], hippocampus [27, 28], transentorhinal cortex [27, 29], and temporal cortex [27, 30], whereas other studies did not describe an increase in the hippocampus [31] or neocortex [32]. Postmortem studies using Iba1 have reported the absence of microglial activity in DLB cases compared to AD cases or controls in the hippocampus [31] and cerebral cortex [30, 32]. Only two post-mortem studies of astroglial activation have reported an increase in GFAP expression in the temporal cortex [33] and pulvinar [34] in DLB cases compared to controls. The inflammatory response in DLB cases with AD co-pathology has not yet been elucidated, although clarifying these pathomechanisms serves several purposes, such as developing biomarkers to improve early diagnosis, predict disease progression, or to discover targets for early disease-modifying drugs [35]. Targeting glial cells has been proposed to be beneficial in early-stage neurodegenerative diseases, as neurodegeneration and neuronal cell death are irreversible and are thought to result from chronic neuroinflammation [36–38].

Recent cerebrospinal fluid (CSF) biomarker studies suggest that inflammation in DLB is related to AD co-pathology and is therefore less pronounced in pure DLB cases [39, 40]. For example, stratification of a DLB group with coexisting AD pathology in the CSF demonstrated higher levels of the glial marker YKL-40 [39], suggesting that the increase is related to AD neurodegeneration. In addition, a post-mortem study described that the number of activated microglial cells in PD was not associated with the number of LBs [41]. Moreover, one postmortem study in DLB reported that biochemical measures of CD200 and ICAM-1 correlated with AD plaque density, and found direct co-localization of microglia with AD plaques rather than with LBs [41, 42]. Interestingly, α-syn accumulation is also observed in activated astrocytes in PD and DLB which may suggest a direct link between α-syn accumulation and activation of the innate immune system [11, 43–45]. In addition, PET imaging studies with 11 C-PK11195, a marker of microglial activation [46], showed significantly higher binding in early DLB cases when compared to those with an advanced disease stage [47, 48]. Likewise, 11 C-PK11195 binding was increased in early AD, suggesting that microglial activation is an early event in both DLB and AD [49, 50]. However, not

all studies distinguish between pure DLB and mixed DLB+AD cases, i.e. cases with mixed DLB and AD pathology, when investigating immune responses, leading to conflicting results.

Several genetic studies highlight the relevance of the immune system in AD and PD. For example, single nucleotide polymorphisms (SNPs) in the HLA genetic loci have been associated with a protective effect for both diseases, and are primarily driven by polymorphisms present in most *HLA-DRB1*04* subtypes [51–53]. In addition, genetic risk factor *APOEε4*, known to increase the presence of AD co-pathology [54], was found to be associated with a greater expression of microglial markers CD68 and HLA-DR and reduced expression of Iba1 [55]. Contrarily, mutations in the glucocerebrosidase (GBA) gene are associated with pathologically pure forms of DLB without AD co-pathology [56]. For that reason, we believe it is important to investigate the frequency of *HLA-DRB1*04*, *APOEε4* and *GBA1* and their effect on pathology and glial load in our cohort.

Our study aims to determine whether there is a different pattern of neuroinflammation in DLB cases with AD co-pathology compared to pure DLB and pure AD cases. In addition, we aim to investigate whether microglial and astroglial activation is associated with α-syn pathology or with AD co-pathology in mixed DLB+AD. Next, we will investigate whether microglial and astroglial activation is higher in regions with a higher burden of α-syn and concomitant p-tau and Aβ pathology. Lastly, we genotyped three common genetic risk genes in DLB and AD, i.e. *GBA1* mutation and frequency of *APOEε4* and *HLA-DRB1*04* alleles, to investigate their effect on pathology burden and inflammatory response in our cohort [52, 56, 57]. To answer these questions, immunostaining, quantitative image analysis, confocal microscopy and genotyping were performed in limbic and cortical brain regions in a cohort of mixed DLB+AD, pure DLB, pure AD and controls.

Methods
Study cohort
For this study, a total of 77 brain donors were included. Postmortem brain tissue from pure AD ($n=16$), pure DLB ($n=15$), mixed DLB+AD ($n=35$) and controls ($n=11$) was obtained from the Netherlands Brain Bank (NBB; Amsterdam, the Netherlands; http://brainbank. nl), and the Normal Aging Brain Collection Amsterdam (NABCA; Amsterdam, the Netherlands; http://nabca. eu). Written informed consent for brain autopsy, the use of the material and the use of clinical information for research purposes was collected from all donors. All procedures of NBB and NABCA were approved by the local ethical board of VU University Medical Center,

Amsterdam. For donor characteristics, see Supplement 1, Additional File 1.

Donors were selected based on clinical and neuropathological diagnosis. The inclusion criteria for a pure DLB diagnosis were (1) a clinical diagnosis of probable DLB according to the DLB consortium criteria [3], (2) the presence of diffuse-neocortical or limbic-transitional α-syn pathology at the time of autopsy (Braak α-syn stage ≥ 4), and 3), AD pathology was absent or low according to the National Institute of Aging-Alzheimer's association (NIA-AA) guidelines [58]. Donors were included in the pure AD group if they met the following criteria: (1) a clinical diagnosis of probable AD and (2) intermediate or high levels of AD pathology [58]. Donors with an atypical clinical AD phenotype, as defined by Boon et al. [59], were excluded. The inclusion criteria for the mixed DLB+AD group were (1) a clinical diagnosis of probable DLB [3], (2) the presence of diffuse-neocortical or limbic-transitional α-syn pathology, and (3) moderate or high levels of AD pathology [58]. The control group was age-matched, and donors were included if there were no records of any neurological disorders. Only donors of which sufficient clinical information for classification and brain tissue samples were available, were included.

Detection of pathology and inflammation with immunohistochemistry
Tissue blocks were collected from the following brain regions: the amygdala, hippocampus (HipMid) and middle temporal gyrus (MTG). Sections were cut at 6–7 μm thickness from formalin-fixed, paraffin-embedded blocks and mounted to glass slides. Immunohistochemistry (IHC) was performed with antibodies against full-length alpha-synuclein (1/500, *clone KM51, Monosan Xtra, The Netherlands*), amyloid-beta (1/500, *clone 70 6F/3D, Dako, Denmark*), and phosphorylated tau (1/500, *p-tau, clone AT8, Thermo Fisher Scientific, USA)* and microglial markers CD68 (1/500, *Mouse monoclonal, Clone KP1, Catalogue No. M0814, DAKO)*, HLA-DR (1/400, Mouse *monoclonal, Clone CR3/43, Catalogue No. M0775, DAKO*), and Iba1 (1/2000, *Goat polyclonal, Catalogue No. ab5076, Abcam)*, and astrocytic marker GFAP (1/1000, *Mouse Anti-GFAP, Catalogue No. G3893, SIGMA)*. See Supplement 2, Additional File 1 for details of the staining protocols.

Microscopic analysis
IHC sections were quantitatively assessed after digitization with the Vectra Polaris Quantitative Pathology Imaging System (PerkinElmer, USA) at 20x magnification. Representative areas [see Supplement 3, Additional File 1] were manually delineated using QuPath software, version 3.0.0 [60], in which the amygdala was delineated as entire amygdaloid complex [61], the hippocampus

annotation was divided into the following subregions: dentate gyrus (DG), cornu ammonis (CA1, CA2, CA3, CA4), subiculum and parasubiculum [62], and the cortical regions (entorhinal cortex (EntC), parahippocampal gyrus (PHG), fusiform gyrus (FusG) and temporal cortex (TC)) had to include all six cortical layers within non-curved areas. All images were analyzed with QuPath open source software [60] using in-house developed scripts [see Supplement 4, Additional File 1], quantifying the percentage of total DAB-stained area, in this study referred to as immunopositivity [see Supplement 5, Additional File 1]. A Color Deconvolution Stains tool in QuPath was used to correct for unspecific background. Besides, images of microglial and astroglial morphology in the amygdala, CA1, CA2 and PHG were shown, based on microscopic assessment at 40x magnification of representative pure and mixed DLB cases. In addition, a semi-quantitative analysis on glial morphology in the amygdala was performed using QuPath software. A grid of 0.25 mm^2 was placed within the area with the highest load of immunopositivity within the amygdala. For microglial morphology, five common microglial structures (homeostatic, reactive, amoeboid, rod-like and clustered microglia) were manually selected and counted within the 0.25 mm^2 grid by QuPath software to calculate the density of the microglial subtype per area. To assess microglial morphology the Iba1 marker was selected, being a pan-marker that stains all microglial structures [63]. Astrocytic morphology was assessed semi-quantitatively in the same manner. Normal physiologic astrocytic structures, reactive astrocytic structures and total GFAP-positive cells were manually selected to calculate the density of the astrocytic subtypes per area. See [Fig. 1] for a schematic representation of the different glial structures, adjusted on the nomenclatures presented in previous papers [64–67].

Multi-labeling immunofluorescence and confocal microscopy

To describe the morphology and co-localization of pathology and microglia, multi-labeling immunofluorescence staining in combination with 3D confocal laser scanning microscopy (CLSM) of microglia (Iba1), phosphorylated α-syn- (p-syn), Aβ- and p-tau-pathology was performed on a Leica TCS SP8 (Leica, Microsystems, Germany). Plaques and their co-localization with microglia were described in four mixed DLB+AD cases in the hippocampus. Images were deconvoluted using standard CLSM algorithms from Huygens Professional (Scientific Volume Imaging; Huygens, The Netherlands; https://svi.nl/Huygens-Professional), and their maximum projections were used to graphically represent structures of interest in ImageJ (ImageJ Fiji, National Institute of Health USA; https://imagej.nih.gov/ij/). Details of the protocol were described in Supplement 2, Additional File 1.

*APOEε4, HLA-DRB1*04* and *GBA1* genotyping

The frequencies of *APOEε4* and *HLA-DRB1*04* subtype alleles and *GBA1* mutations were determined by genotyping using either the Infinium® NeuroChip Consortium Array v1.1 (Illumina) or Sanger sequencing (Invitrogen
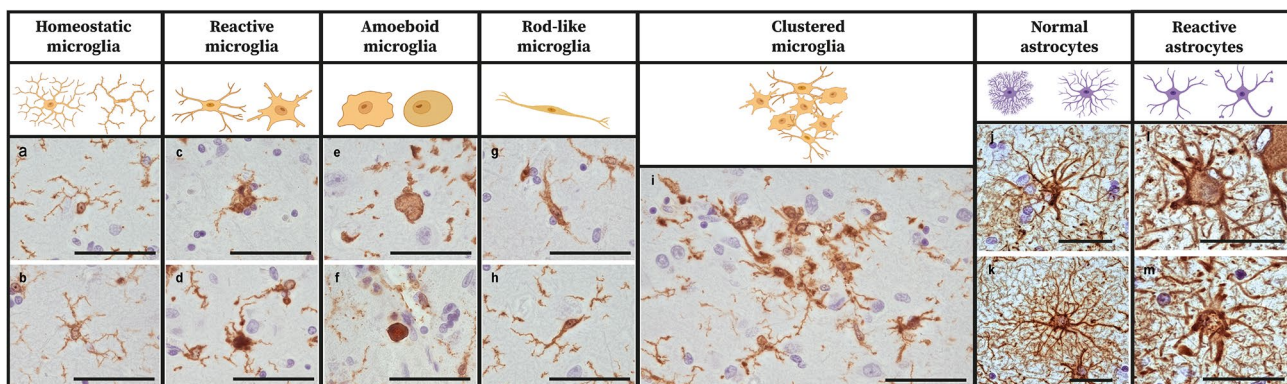

Fig. 1 The morphology of microglial and astrocytic structures in the amygdala. Schematic drawings of the common morphological microglial and astrocytic structures including representative immunostained images of these morphological subtypes in the amygdala. Morphological nomenclature is stated as derived from the previous papers [64–67]. Immunostaining was performed with microglial marker Iba1 for images **a-i** and with astrocytic marker GFAP for images **j-m**. Homeostatic microglia have a small soma and long complex processes as shown in a control donor (**a**) and a pure DLB case (**b**). Reactive microglia show a larger soma with retracted and fewer processes as demonstrated in a mixed DLB+AD (**c**) and pure AD (**d**) case. Amoeboid microglia typically lack processes and have a large soma, here demonstrated in a pure AD (**e**) and control donor (**f**). Rod-like microglia are characterized by a long thin soma with long extended processes, shown here in a pure DLB case (**g**) and a control donor (**h**). Clustered microglia are characterized by the proximity of multiple microglial somas, and mostly consist of amoeboid and reactive microglial cells. An example of a large microglial cluster is shown in a pure AD case (**i**). Normal physiologic astrocytes have a small cell soma with long, thin and complex processes as shown in a pure DLB case (**j**) and a control donor (**k**). Reactive astrocytes have a larger cell soma with short, retracted and large processes as shown in a pure AD case (**l, m**). Scale bar represents 50 μm in each image

Life Technologies, Carlsbad, CA, USA). Details of the NeuroChip and Sanger sequencing methods used were described in previously published studies by Tunold et al. [68] and Moors et al. [69], respectively. *HLA-DRB1*04* alleles were imputed from genotypes using the SNP2HLA software package with publicly available reference data from the Type 1 Diabetes Genetics Consortium [70]. The primer sequences are available upon request.

Statistical analysis

All the statistical analyses were performed in IBM SPSS Statistics version 28. Demographics between disease groups were compared using a one-way ANOVA with post-hoc t-tests for continuous variables and a Fisher's exact test with post-hoc pairwise comparisons for categorical variables. A linear mixed model analysis adjusted for age at death and sex was performed to estimate differences in glial morphological density of Iba1 and GFAP and to estimate immunoreactivity of each IHC marker (α-syn, Aβ, p-tau, Iba1, HLA-DR, CD68 and GFAP) between disease groups within the different regions and between different genotypes. To estimate differences in immunoreactivity between brain regions over all groups, a correction for disease group was added to the analysis. Associations between the various neuroinflammatory markers (Iba1, HLA-DR, CD68 and GFAP) and pathology markers (α-syn, Aβ and p-tau) were analyzed using a linear mixed model correcting for age at death and sex. Pathology or neuroinflammatory marker analysis was further adjusted for α-syn load, Aβ load or p-tau load. Based on the results of the linear mixed model analysis, standardized regression coefficients (r) were calculated for the four diagnostic groups. Significance for all analyses was based on p-values < 0.05 after FDR-correction for multiple comparisons, with subsequent reporting of FDR-corrected p-values [71]. Heatmaps and graphs were generated using GraphPad Prism version 9.3.1 (Graph-Pad Software, San Diego, California, USA).

Results

Demographics of the cohort

A shorter survival time between disease diagnosis and death was observed in mixed DLB+AD (6±3 years) than in pure DLB (8±3 years; *p*=0.030) and pure AD (10±5 years; *p*<0.001) cases [Table 1]. Higher Braak stages for neurofibrillary tangles (NFT) (*p*=0.003), Thal stages for Aβ (*p*<0.001) and Consortium to Establish a Registry for Alzheimer's Disease (CERAD) scores (*p*<0.001) were observed in pure AD when compared to mixed DLB+AD cases. No significant difference in Braak stage for α-syn was observed between pure DLB and mixed DLB+AD cases. Heterozygous and homozygous *APOEε4* were more frequent in mixed DLB+AD (9% non-carriers, 79% heterozygous and 12% homozygous) than in pure DLB

(62% non-carriers, 38% heterozygous and 0% homozygous; *p*<0.001) and controls (73% non-carriers, 27% heterozygous and 0% homozygous; *p*<0.001), but did not significantly differ with pure AD cases (31% non-carriers, 56% heterozygous and 13% homozygous). A higher frequency of *GBA1* mutations, varying in risk variant [see Table 1], was observed in pure DLB cases (62%) compared to mixed DLB+AD cases (12%) (*p*<0.001). There were no significant differences in the frequency of *HLA-DRB1*04* alleles between diagnostic groups.

Regional differences in pathological load across diagnostic groups

For all cases, the pathological loads of α-syn, Aβ and p-tau were assessed in cortical regions (EntC, PHG, FusG and TC), the amygdala and hippocampus (CA1-4, DG, subiculum and parasubiculum) [Fig. 2]. Mixed DLB+AD cases had a higher α-syn load in the amygdala (*p*=0.017) compared to pure DLB cases. The Aβ load was similar in mixed DLB+AD and pure AD cases, and was only higher in the TC of pure AD cases (*p*=0.001). Higher p-tau loads were found for pure AD cases when compared to mixed DLB+AD cases in the amygdala, subiculum and FusG (*p*=0.002, *p*=0.001, *p*=0.004, respectively), and did not differ in other regions. By design, mixed DLB+AD cases had higher loads of AD-pathology than pure DLB cases and higher loads of α-syn than pure AD cases [see comparisons in Supplement 6, Additional File 1]. Across groups, the highest α-syn load existed in the CA2, and was significantly higher than in all the other brain regions examined (*p*<0.001).,The highest Aβ load was found in cortical regions and was significantly higher in the EntC, PHG, FusG and TC than in the DG, CA1-4, subiculum and amygdala (all *p*<0.001). Similar to the α-syn load, the highest p-tau load was found in the CA1 and CA2 and was higher when compared to the DG, CA3, CA4, amygdala, subiculum, parasubiculum, EntC, FusG and TC (all *p*<0.001). Additional regional differences in α-syn, Aβ and p-tau loads are stated in Supplement 7, Additional File 1.

Mainly amoeboid and reactive microglial structures and physiologic astrocytes in the amygdala of mixed DLB cases

As previously described, the amygdala is a region suggested to be prone to start pathological misfolding of α-syn, Aβ and p-tau pathology [11, 12]. In addition, after the CA1 and CA2 region, where mostly neurites and a few plaques were observed, the highest α-syn, p-tau and microglial load and a wide variety of pathological structures existed in the amygdala in our cohort [see Supplement 7, Additional File 1]. Therefore, we decided to describe and count microglial and astrocytic structures in the amygdala for all groups [see Fig. 1+3]. Group differences in the density of different morphological structures

Table 1. Group demographics, neuropathological stages and genotype of study cohort

	Controls	Pure AD	Pure DLB	Mixed DLB+AD	P-value [1]
N	11	16	15	35	
Sex					n.s.
M/F (%M)	4/11 (36%)	11/16 (69%)	12/15 (80%)	23/35 (66%)	
Age at onset					n.s.
y mean ± SD (range)	n.a.	65 ± 10 (48-84)	67 ± 8 (53-79)	69 ± 8 (50-81)	
Age at death					n.s.
y mean ± SD (range)	70 ± 7 (59-79)	75 ± 11 (53-92)	76 ± 8 (61-90)	75 ± 8 (56-87)	
Disease duration					$p < 0.001$ E
y mean ± SD (range)					$p = 0.030$ F
	n.a.	10 ± 5 (2-23)	8 ± 3 (3-13)	6 ± 3 (2-14)	n.s. D
Braak NFT [6]					$p < 0.001$ A,C,D,F
0/1/2/3/4/5/6	3/6/2/0/0/0/0	0/0/0/0/3/6/7	0/7/8/0/0/0/0	0/0/0/3/21/9/2	$p = 0.003$ E
					$p = 0.044$ B
Thal Aβ [9]					$p < 0.001$ A,C,D,E,F
0/1/2/3/4/5/6	3/3/3/2/0/0/0	0/0/0/1/5/10/0	5/2/4/4/0/0/0	0/0/1/12/22/0/0	n.s. B
Braak α-syn [72]					$p < 0.001$ B,C,D,E
0/1/2/3/4/5/6	10/0/0/0/0/0/0	16/0/0/0/0/0/0	0/0/0/0/0/2/13	0/0/0/0/0/6/29	n.s. A,F
CERAD [73]					$p < 0.001$ A,C,D,E,F
0/1/2/3	11/0/0/0	0/0/4/12	9/5/1/0	0/15/12/8	$p = 0.029$ B
CAA [18]					$p < 0.001$ A,C,F
0/1/2/3	8/1/1/0	0/12/3/0	7/4/4/0	0/21/12/2	$p = 0.003$ D
					n.s. B,E
***APOEε4*, n/N (%)**					
Non-carrier	8/11 (73%)	5/16 (31%)	8/13 (62%)	3/33 (9%)	$p < 0.001$ C,F
Heterozygous	3/11 (27%)	9/16 (56%)	5/13 (38%)	26/33 (79%)	n.s. A,B,D,E
Homozygous	0/10 (0%)	2/16 (13%)	0/13 (0%)	4/33 (12%)	
***HLA-DRB1*04*, n/N (%)**					n.s.
Negative	6/10 (60%)	n.a.	9/13 (69%)	25/28 (89%)	
Monoallelic	3/10 (30%)		4/13 (31%)	2/28 (7%)	
Biallelic	1/10 (10%)		0/13 (0%)	1/28 (4%)	
***GBA1* mutations, n/N (%)**	n.a.	n.a.	8/13 (62%)	4/33 (12%)	$p = 0.001$
E326K			3	2	
V460M			0	1	
T369M			3	2	
N370S			2	0	

Table 1 Group demographics, neuropathological stages and genotype of study cohort

were estimated with a linear mixed model analysis with correction for age at death and sex. The density of homeostatic microglia, characterized by a small soma and long complex processes, was significantly higher in controls than in mixed DLB+AD, pure AD ($p < 0.001$ in both) and pure DLB ($p = 0.01$), and in pure DLB than in mixed DLB+AD and pure AD cases ($p < 0.001$). In contrast, the density of reactive microglia, characterized by a large soma and short retracted processes, was higher in pure AD than in pure DLB ($p = 0.002$) and controls ($p < 0.001$) and in mixed DLB+AD than in pure DLB and controls ($p < 0.001$ in both). Likewise, the density of amoeboid microglia, characterized by a large round soma without processes, was higher in pure AD than in pure DLB, controls ($p < 0.001$ in both) and mixed DLB+AD (p 0.002), and in mixed DLB+AD than in pure DLB

($p = 0.005$) and controls ($p = 0.026$). No differences in rod-like microglia, characterized by a long, thin soma and long but simple processes, existed between groups. The density of clustered microglia in the amygdala was higher in pure AD cases than in all other groups ($p < 0.001$ in all). The density of normal physiologic astrocytes, characterized by a small soma and long complex processes, was higher in mixed DLB+AD than in pure AD ($p < 0.001$) and controls ($p = 0.002$), and in pure DLB than in pure AD ($p = 0.012$). In contrast, the density of reactive astrocytes, characterized by a large soma with short retracted processes, was higher in pure AD cases than in all other groups ($p < 0.001$ in all). Total GFAP-positive astrocytic density, which is suggested to characterize astrocytic reactivity [66], was higher in pure AD than in pure DLB cases ($p = 0.003$) or controls ($p < 0.001$).
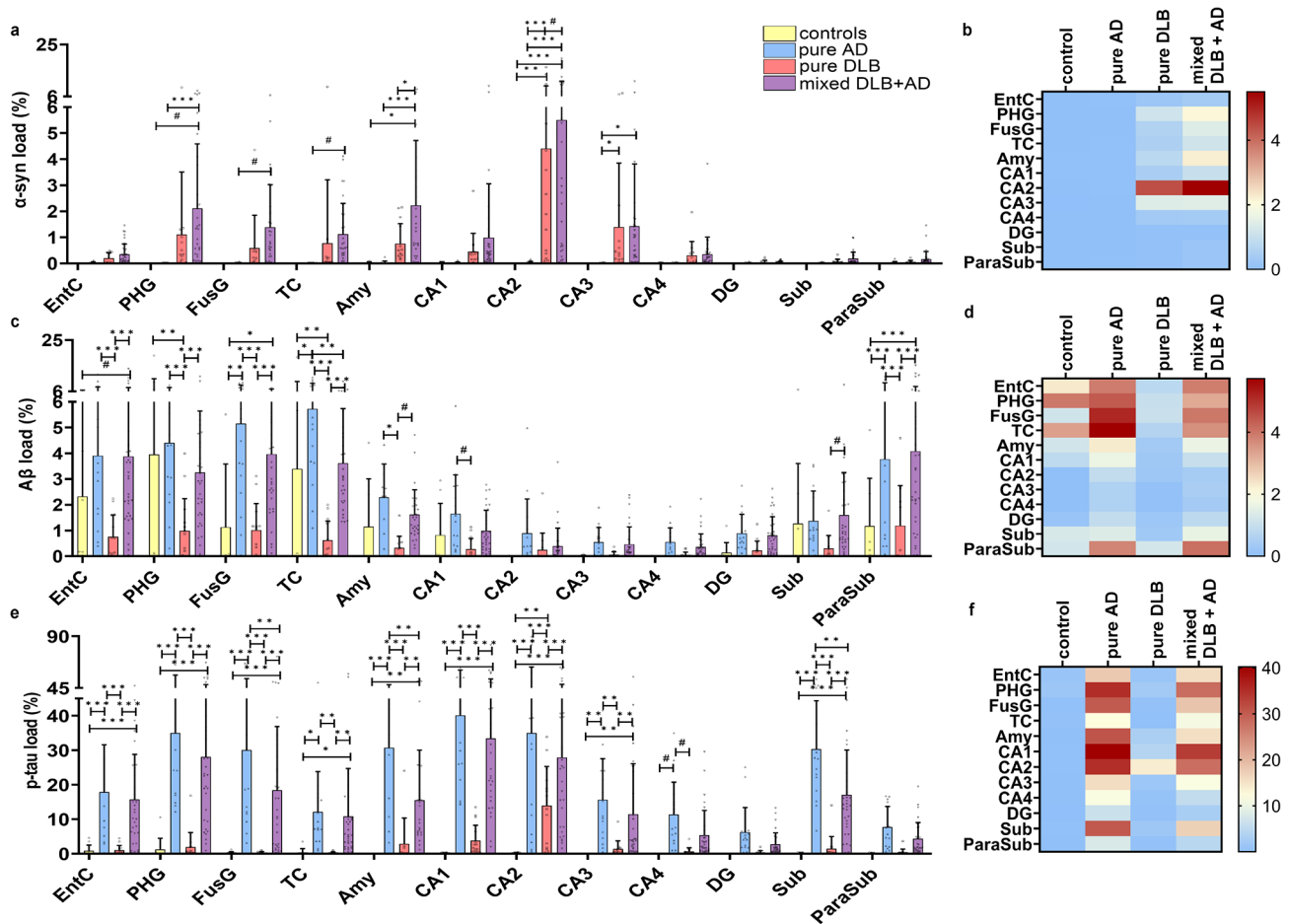
Fig. 2 **Distribution patterns of pathology in limbic and neocortical brain regions across diagnostic groups.** Distribution of α-syn, Aβ and p-tau pathology is visualized in a scatter plot with box and heatmaps of mean pathological load [SD] in which the color-coded legend on the right indicates the %area of pathology. **a-c** α-Syn load was higher in the amygdala of mixed DLB + AD cases than in pure DLB cases. **d-f** Aβ pathology was higher in the TC of pure AD than mixed DLB + AD cases. **g-i** p-Tau was higher in the FusG, amygdala and subiculum of pure AD than mixed DLB + AD cases. A linear mixed model analysis with correction for age at death and sex was performed to estimate group differences. * $p < 0.05$, ** $p < 0.01$, *** $p < 0.001$, # $p < 0.05$ without significance after correction for multiple comparisons. EntC = entorhinal cortex; PHG = parahippocampal gyrus; FusG = fusiform gyrus; TC = temporal cortex; Amy = amygdala; CA = cornu ammonis; DG = dentate gyrus; Sub = subiculum; ParaSub = parasubiculum

Second, differences in glial morphology were described for the amygdala, CA1 and PHG in mixed DLB + AD and pure DLB cases [see Supplement 8, Additional File 1]. Only small differences in microglial structures between regions were observed, but in limbic regions, particularly the amygdala, microglia seemed to be more often in a morphologically reactive state. Astrocytes in the PHG and CA1 seemed to have a larger soma with shorter processes, while astrocytes in the amygdala had a smaller soma with long processes. However, it is important to note that a semi-quantitative assessment was only performed for the amygdala.

Microglial response in mixed DLB is more severe than in pure DLB

Iba1 is located at the outer membrane and is a pan-marker that stains all present microglia including their processes [63], and will be referred to as 'total microglia' throughout this paper. CD68 is mostly expressed by lysosomes and demonstrates round microglial structures without processes, while HLA-DR is located at the cytoplasm. Both CD68 and HLA-DR are markers that are mostly upregulated in phagocytosing and thus reactive microglia and foamy macrophages [74], and will be referred to as 'reactive microglia'. However, it should be noted that not only reactive, but also homeostatic microglia will be stained by CD68 and HLA-DR. Total microglial (Iba1-positive) and reactive microglial (CD68- and HLA-DR-positive) loads were quantified within the amygdala, hippocampal subregions and cortical regions [Fig. 4]. The total microglial load (Iba1-positive), observed in the control group, was higher in the amygdala when compared to pure AD, pure DLB and mixed DLB + AD ($p = 0.016$, $p < 0.001$, $p = 0.002$, respectively),
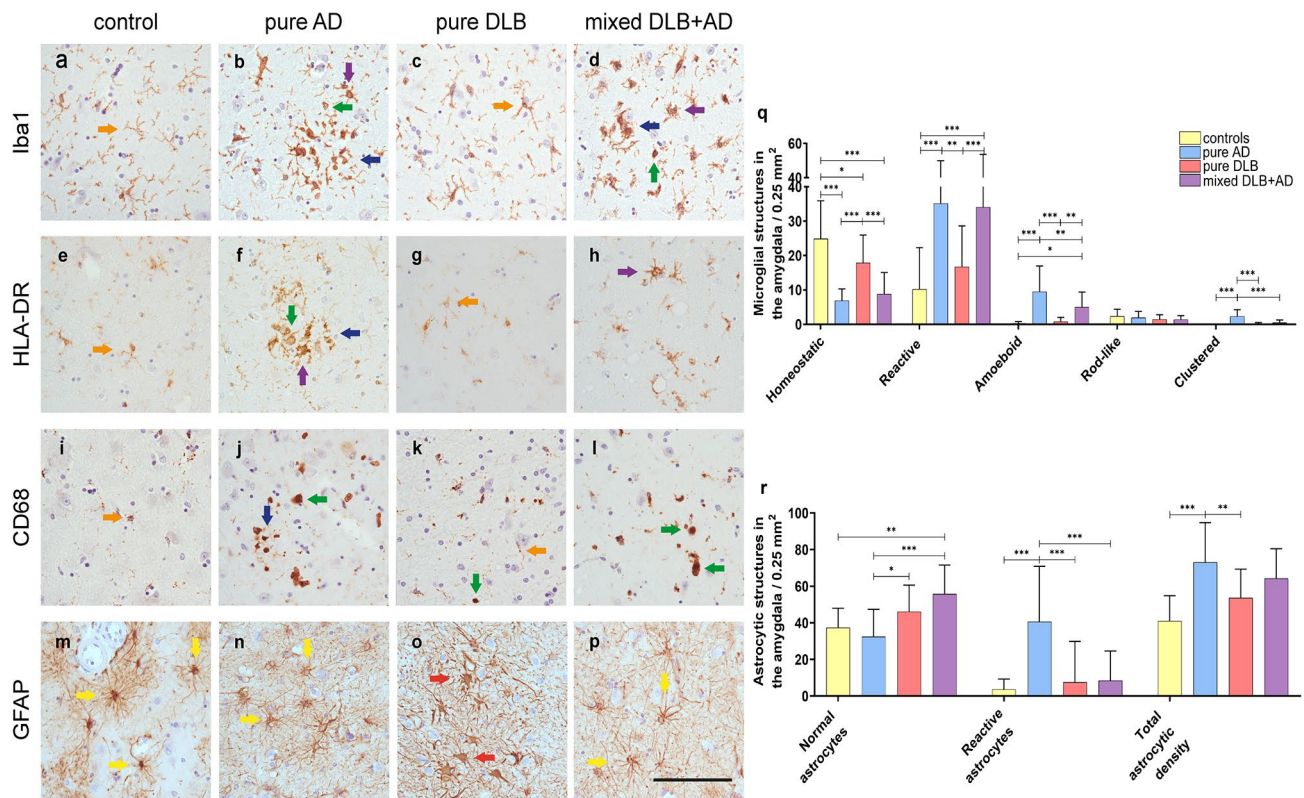
Fig. 3 Amoeboid and reactive microglial morphology and physiologic astrocytic morphology in mixed DLB cases. Representative images of microglial (**a-l**) and astrocytic (**m-p**) morphology in the amygdala with a scatter plot of the mean density of microglial Iba1-positive (**q**) and astrocytic (**r**) structures in the amygdala [SD]. **a, e, i** In control cases, homeostatic microglia with long processes (orange arrowhead) were observed. **b, f, j** In pure AD cases, amoeboid microglia with a large and round soma (green arrowhead), reactive microglia with short retracted processes (purple arrowhead) and clustered microglia (blue arrowhead) were observed. **c, g, k** In pure DLB cases, homeostatic (orange arrowhead) microglia and small amoeboid microglia (green arrowhead) were observed. **d, h, l** Mixed DLB + AD cases demonstrated amoeboid (green arrowhead), reactive (purple arrowhead) and clustered microglia (blue arrowhead). **m, n, p** In control, pure DLB and mixed DLB + AD cases normal physiologic astrocytes with a small soma and long, thin, complex processes (yellow arrowhead) were observed. **o** A higher total astrocytic density and reactive astrocytes with a swollen soma and short retracted processes (red arrowhead) were observed in pure AD cases. **q** The density of homeostatic microglia in the amygdala was significantly higher in control and pure DLB cases than in mixed DLB + AD and pure AD cases. The density of reactive and amoeboid microglia in the amygdala was higher in mixed DLB + AD and pure AD cases than in pure DLB and control cases. The density of clustered microglia in the amygdala was higher in pure AD cases than in all other groups. **r** The density of normal astrocytes was higher in mixed DLB + AD and pure DLB cases than in pure AD and controls, while the density of reactive astrocytes was higher in pure AD cases than in all other groups in the amygdala. Total astrocytic density in the amygdala was higher in pure AD than in pure DLB cases or controls. Scale bar in **p** is identical for all images and represents 100 μm

in the DG, CA3 and CA4 when compared to mixed DLB+AD ($p=0.045$, $p=0.012$, $p=0.015$, respectively) and in the CA4 when compared to pure DLB ($p=0.012$). Pure AD cases showed a higher load of total microglia in the CA1 and CA2 when compared to pure DLB cases ($p=0.012$, $p=0.042$) and to mixed DLB+AD cases ($p=0.021$, $p=0.027$). No differences in total microglial load were observed between mixed and pure DLB cases. Across all groups, the highest total microglial load was found in the CA2, which was significantly higher than in all the other brain regions assessed ($p<0.001$).

Second, reactive microglia were examined [63, 74]. In [Fig. 4c-d], mixed DLB+AD and pure AD cases appeared to have a higher reactive microglial load (HLA-DR-positive) in the amygdala, CA1 and subiculum than pure DLB cases. However, after correction for multiple comparisons, no statistical significant differences in reactive microglial loads (HLA-DR-positive) were observed between groups. We then analyzed the reactive microglial load (HLA-DR-positive) between regions and found that it was the highest in the amygdala when compared to all other regions (all $p<0.001$). As shown in [Fig. 4e-f], a high reactive microglial load (CD68-positive) was observed in limbic regions of mixed DLB+AD and pure AD cases. Reactive microglial load (CD68-positive) was significantly higher in mixed DLB+AD cases compared to pure DLB cases in the amygdala and PHG ($p<0.001$ and $p=0.004$ respectively), in pure AD cases when compared to pure DLB cases in the CA1, CA2, the subiculum and amygdala ($p=0.004$, $p=0.028$, $p=0.002$, $p<0.001$, respectively) and in pure AD cases when compared to mixed DLB+AD cases in the CA2 and subiculum
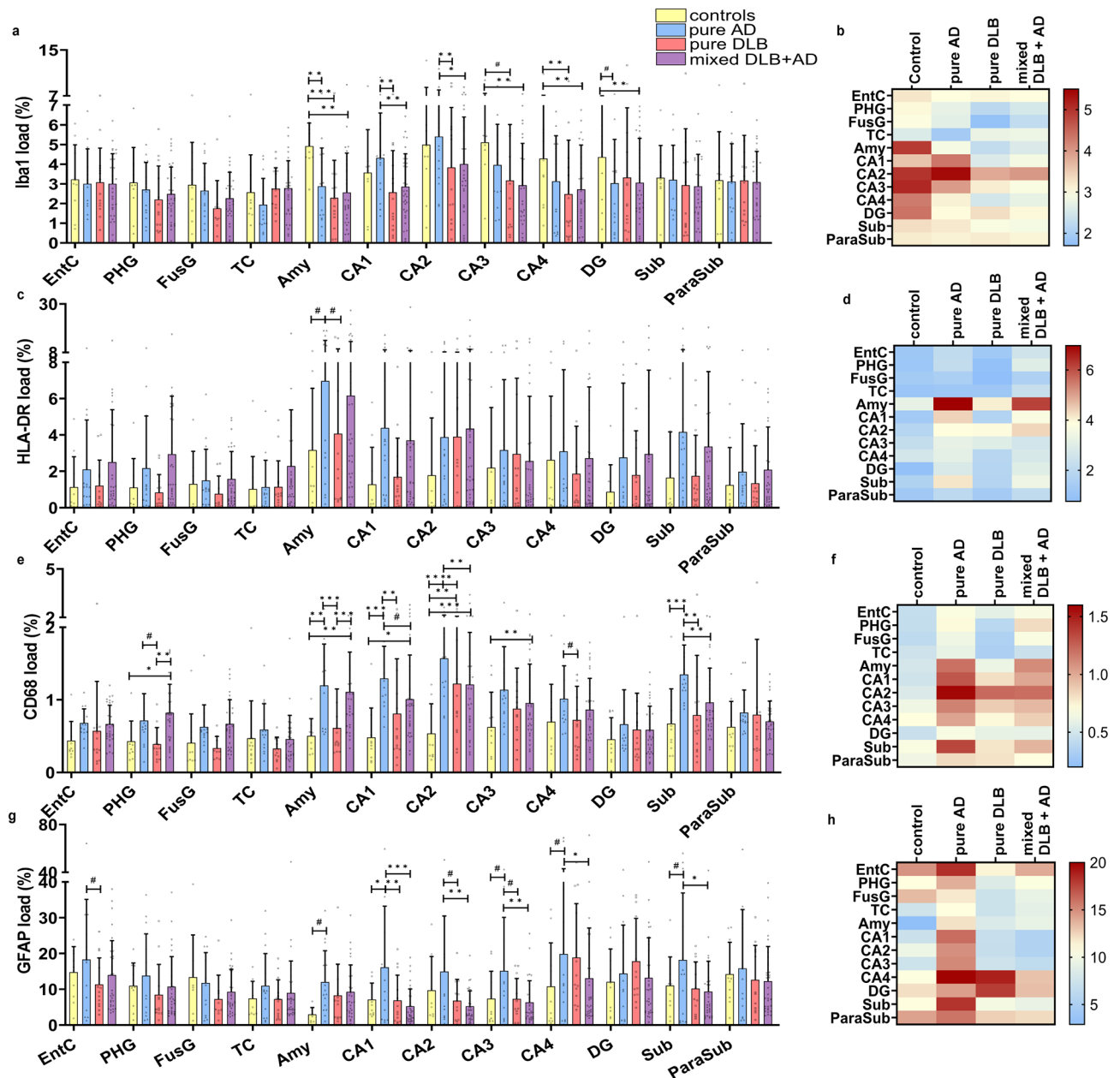
Fig. 4 **Microglial response was more severe in mixed DLB cases, while astrocytic response was similar to pure DLB.** Distribution patterns in regions of interest are visualized in a scatter plot with box and heatmaps of mean microglial load [SD], in which the color-coded legend on the right indicates the %area of immunopositivity. **a-c** Iba1-positive microglial load was higher in controls than in pure AD in the amygdala, than in pure DLB in the amygdala and CA4, and higher than in mixed DLB+AD in the amygdala, CA3, CA4 and DG. **d-f** The highest reactive microglial load, measured by HLA-DR, was observed in the amygdala of mixed DLB+AD and pure AD cases, but was not significantly higher after correction for multiple comparisons. **g-i** Mixed DLB+AD showed a higher reactive microglial load, as measured by CD68, than pure DLB in the PHG and amygdala. Pure AD had a higher CD68 positive microglial load than mixed DLB+AD in the CA2 and subiculum. **j-l** Pure AD cases had a higher astrocytic load in the CA1, CA2, CA3, CA4 and subiculum than mixed DLB+AD cases. A linear mixed model analysis with correction for age at death and sex was performed to estimate group differences. * $p < 0.05$, ** $p < 0.01$, *** $p < 0.001$, # $p < 0.05$ without significance after correction for multiple comparisons. EntC = entorhinal cortex; PHG = parahippocampal gyrus; FusG = fusiform gyrus; TC = temporal cortex; Amy = amygdala; CA = cornu ammonis; DG = dentate gyrus; Sub = subiculum; ParaSub = parasubiculum

($p=0.01$ and $p=0.014$ respectively). The highest reactive microglial load (CD68-positive) was found in the CA2 and was higher than in all other regions (all $p<0.001$).

Astrocytic response in mixed and pure DLB cases is similar

GFAP is a marker that becomes upregulated in reactive astrocytes [75] and was quantified within the amygdala, hippocampal subregions and cortical regions [Fig. 4g-h]. A significantly higher astrocytic load (GFAP-positive) was observed in pure AD cases than in mixed DLB+AD in the CA1, CA2, CA3, CA4 and subiculum ($p<0.001$, $p=0.003$, $p=0.01$, $p=0.042$, $p=0.006$ respectively) and in pure DLB in the CA1 ($p=0.014$). No differences in astrocytic load were observed between mixed and pure DLB cases. In contrast with the abundance of α-syn and p-tau pathology and microglial load, we observed the lowest astrocytic load in the amygdala, CA1 and CA2 when compared to other regions. The highest astrocytic load was found in the CA4 compared to the PHG, FusG, TC, amygdala, CA1, CA2, CA3 ($p<0.001$ in all) and subiculum ($p=0.002$). Additional regional differences in Iba1, HLA-DR, CD68 and GFAP loads are shown in Supplement 7, Additional File 1.

Microglial response in close proximity to AD plaques in mixed DLB cases

When we studied the spatial relationship between microglia and plaques with multi-labeled immunofluorescence for Iba1, Aβ, p-tau and p-syn staining (pSer129), many large clustered and amoeboid Iba1-positive microglia were observed in and surrounding neuritic plaques consisting of Aβ and p-tau pathology [Fig. 5a, f, k]. We showed neuritic and classical dense-cored plaques as previously described by Walker et al., derived from the preceding description by Thal et al. [76, 77]. One image showed a large amoeboid Iba1-positive microglial cell with a large cell soma completely within a classic cored plaque that mainly consisted of Aβ and p-tau pathology [see Fig. 5p-t]. Direct co-localization between LBs or LNs and Iba1-positive microglia was not found. However, punctate p-syn, which can be either astrocytic, neuritic or synaptic α-syn, was present in the AD-plaques.

Whereas microglia associated with AD-, astroglia associated with amygdalar α-syn-pathology in mixed DLB

Standardized regression coefficients between microglial and astroglial, and α-syn, Aβ and p-tau load were assessed for each group over all regions, with adjustments for age at death, sex and α-syn, Aβ and p-tau loads [see Table 2]. The α-syn load in pure AD cases and controls was negligible, hence these associations were not described. Total microglial load (Iba1-positive), associated negatively with Aβ load in pure AD and mixed DLB+AD ($r = -0.40$, $p<0.001$; $r = -0.11$, $p=0.012$) and

positively with p-tau load in pure AD ($r=0.18$, $p=0.021$). Reactive microglial load (HLA-DR-positive) correlated negatively with Aβ load in pure AD, pure DLB and mixed DLB+AD ($r = -0.13$, $p=0.033$; $r = -0.16$, $p=0.048$; $r = -0.15$, $p<0.001$) and positively with p-tau load in pure AD, pure DLB and mixed DLB+AD ($r=0.24$, $r=0.28$ and $r=0.12$, $p<0.001$). Reactive microglial load (CD68-positive), again associated negatively with Aβ load in pure AD and mixed DLB+AD ($r = -0.36$ and $r = -0.21$, $p<0.001$) and positively with p-tau load in pure AD, pure DLB, and mixed DLB+AD ($r=0.38$, $r=0.30$ and $r=0.28$, $p<0.001$). Astrocytic load was not associated with pathological load in the assessed diagnostic groups.

We then examined associations between microglial and astroglial and α-syn, Aβ and p-tau load within each region in mixed DLB+AD cases to see whether regional differences could be highlighted [see Supplement 9, Additional File 1]. Strong associations between reactive microglial load (CD68-positive), and p-tau load were observed in the PHG and TC ($r=0.41$, $p=0.048$; $r=0.72$, $p<0.001$). Reactive HLA-DR-positive microglial load associated positively with the α-syn load in the CA1 ($r=0.53$, $p=0.024$). Interestingly, astrocytic load showed a strong association with α-syn load in the amygdala ($r=0.69$, $p<0.001$).

More AD-pathology and microglial response in *APOEε4* carriers and less AD-pathology in *GBA1* carriers

Stratification of the frequency of *APOEε4* and *HLA-DRB1*04 alleles and the presence or absence of pathogenic *GBA1* genotypes was performed to examine differences in microglial, astroglial and pathological loads between genetic variants [see Fig. 6]. The observed Aβ load was higher in heterozygous ($p=0.006$) and homozygous ($p=0.006$) *APOEε4* carriers than in non-carriers. In contrast, pathogenic *GBA1* mutation carriers had lower loads of Aβ and p-tau pathology than non-carriers did ($p=0.028$, $p=0.030$). Interestingly, homozygous *APOEε4* carriers had a higher reactive microglial load (CD68-positive) than heterozygous *APOEε4* ($p=0.015$) or non-carriers ($p=0.036$). No significant differences in microglial, astroglial or pathological load were observed between the other genetic variants.

Discussion

Microglial reactivity in DLB associated strongly with Aβ and p-tau loads, while no association with astrocytic response was observed. Morphologically, amoeboid and reactive microglia were abundant in mixed DLB+AD and pure AD cases, while pure DLB and control cases mainly revealed homeostatic microglia and small astrocytes with thin processes. Reactive microglial load was higher in mixed DLB+AD compared to pure DLB cases, but DLB phenotypes, i.e. pure and mixed DLB cases, did not differ
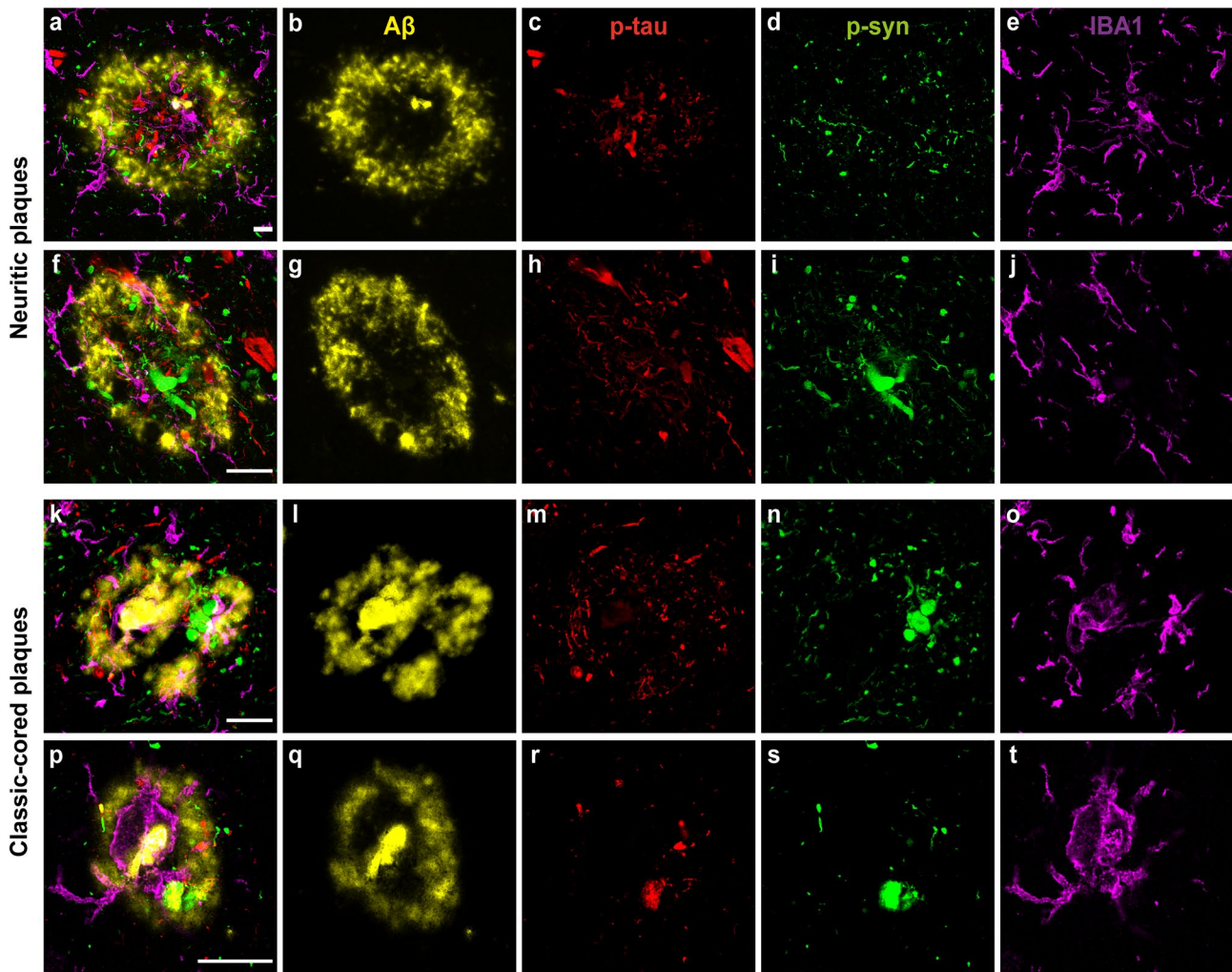
Fig. 5 Representative confocal microscopy images of microglia in close proximity to AD-plaques in mixed DLB cases. Localization of pSer129-syn (green), Aβ (yellow), p-tau (red) and Iba1+ (purple) microglia in neuritic and classic cored plaques in the CA1, EntC and TC regions demonstrated with confocal microscopy. **a-e** Many large clustered and amoeboid Iba1-positive microglia with short, thick processes in the neuritic plaque in the CA1 within and in closer proximity to neuritic p-tau and p-syn accumulation. **f-j** Another example of rod-like and amoeboid Iba1-positive microglia in a neuritic plaque in the CA1. **k-o** Amoeboid and clustered microglia within and surrounding a classic-cored plaque in the EntC with neuritic p-tau and p-syn pathology. **p-t** Reactive microglial cell with large cell soma and thick processes within a classic-cored plaque with mainly Aβ pathology present in the TC. The scale bars in **a, f, k, p** are identical for all images in one row and represent 20 µm in all

x	Controls			pure AD			pure DLB			Mixed DLB+AD		
	α-syn	Aβ	p-tau	α-syn	Aβ	p-tau	α-syn	Aβ	p-tau	α-syn	Aβ	p-tau
IBA1	0.09	-0.17	0.03	0.02	**-0.40*** **	**0.19***	0.11	-0.03	0.11	0.07	**-0.10***	0.06
HLA-DR	**0.18*** **	-0.18	-0.01	-0.04	**-0.12***	**0.23*** **	0.02	**-0.17***	**0.30*** **	0.05	**-0.15*** **	**0.12*** **
CD68	-0.08	-0.23	-0.01	0.09	**-0.36*** **	**0.38*** **	0.05	-0.03	**0.30*** **	**0.17*** **	**-0.22*** **	**0.29*** **
GFAP	-0.44	-0.13	0.17	**-0.13***	0.03	-0.03	-0.07	-0.04	-0.00	-0.03	0.05	-0.10

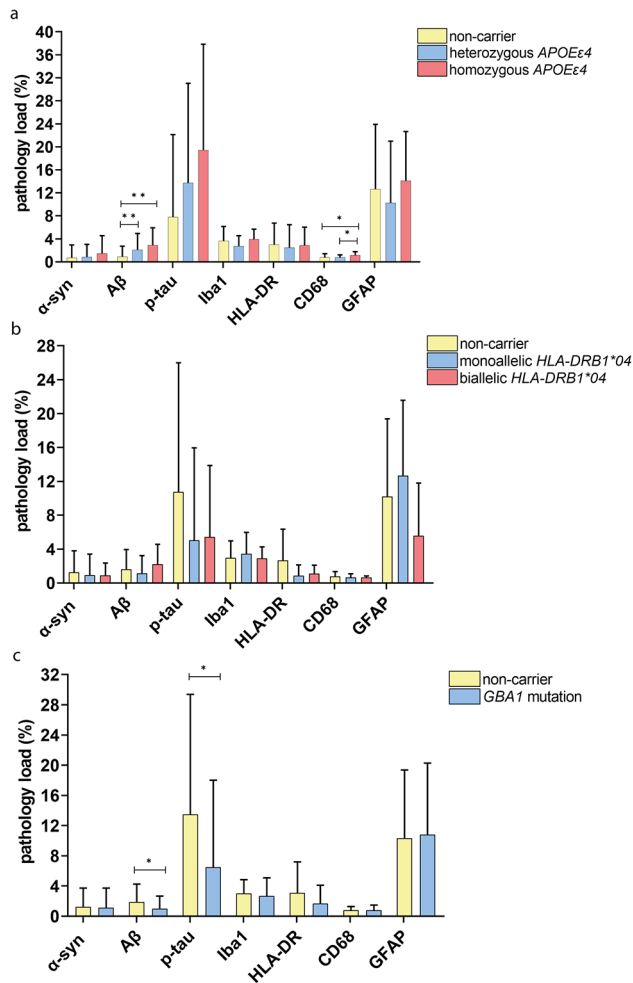**Table 2** Strong associations between microglial load and AD pathology existed in disease groups

Fig. 6 **Variants of *APOEε4* and *GBA1* genotype influenced the level of Aβ and p-tau pathology.** Immunopositivity of α-syn, Aβ, p-tau, Iba1, HLA-DR, CD68 and GFAP is visualized in a scatter plot with box of mean pathology load over all measured brain regions [SD]. **a** Aβ load increased with the number of *APOEε4* alleles and was significantly higher in heterozygous and homozygous than non-carriers. Microglial load was higher in homozygous than in heterozygous *APOEε4* or than in non-carriers. **b** No differences in pathology or micro- or astroglial load were observed between different frequencies of *HLA-DRB1*04 alleles. **c** Pathogenic *GBA1* carriers had a higher Aβ and p-tau load than non-carriers. A linear mixed model analysis with correction for age of death and gender was performed to compare genotypes. * *p* < 0.05, ** *p* < 0.01, *** *p* < 0.001

in astrocytic load. Finally, the highest microglial activity was found in the CA2 and amygdala, where concomitant α-syn and p-tau pathology also showed the highest loads.

Although we observed higher α-syn loads both in cortical regions and the amygdala in mixed DLB+AD cases than in pure DLB cases, which is consistent with previous studies [78–80], significance was only reached in the amygdala in our cohort. These findings suggest that the mixed DLB+AD cases are in a more advanced pathological stage of disease, according to the pattern of α-syn pathology distribution by Braak et al. [81]. However, DLB phenotypes were scored as Braak α-syn stage 5 or 6 and

were not significantly different. This may be explained by the fact that Braak staging does not require evaluation of lesional density and assesses the presence of LBs and LNs [81], whereas we assessed a quantitative measure of total α-syn pathology. We showed that α-syn load was associated with reactive CD68-positive microglial load only in mixed DLB+AD cases. While several cell-culture and animal studies demonstrated a direct link between α-syn and microglial activation [37], few post-mortem studies were able to show this association in the cingulate cortex of PD [27], and in the transentorhinal cortex of pure and mixed DLB cases [29]. Furthermore, double-staining of HLA-DR microglia and α-syn only showed an association with 20% of the LBs in the cingulate cortex of PD [27], and it has been suggested that LBs alone are not sufficient to activate microglia [37]. Moreover, α-syn load strongly associated with astrocytic response in the amygdala in our cohort, a region where astrocytic α-syn was previously reported to be predominant [11]. In addition, the presence of astrocytic α-syn in the amygdala and other brain regions has recently been demonstrated by studying various post-translational modifications (PTMs) of α-syn [43]. These observations suggest that reactive microglia and astrocytes might partly respond to the increase of α-syn pathology in mixed DLB+AD cases, or contribute to a more aggressive synucleinopathy.

As previously described and confirmed by our study, early affected regions in AD exhibited similar Aβ- and p-tau- pathological loads in pure AD and mixed DLB+AD cases [4], while regions affected in more advanced disease stages [6], such as limbic regions for p-tau and cortical regions for Aβ pathology, were more heavily affected in pure AD cases [4, 82]. The presence of p-tau did show a positive association with reactive microglial load for pure AD, pure DLB and mixed DLB+AD. Likewise, a recent study using 3D confocal microscopy demonstrated that p-tau was associated with microglial morphological features in the hippocampus of DLB and AD donors [21]. Interestingly, we observed an overall negative association between Aβ pathology (including diffuse plaques) and microglial load in pure AD and mixed DLB+AD cases. Previous studies have indicated that microglia are able to engulf extracellular fibrillary Aβ plaques [83]; therefore, a negative association was expected. However, we observed that the association between Aβ pathology and reactive microglial load varied in different brain regions within mixed DLB+AD cases. A negative association was observed in the cornu ammonis, a region with a low Aβ load, while the association was reversed in cortical regions. Early microglial activation in AD has been shown to play a role in the phagocytosis of fibrillary Aβ plaques and precedes a pro-inflammatory harmful state of microglia in later disease stages [84]. These findings suggest that reactive microglia

are able to successfully engulf and clear fibrillary Aβ plaques in regions that are affected only in later disease stages [84], such as the cornu ammonis, and that an overload of unengaged fibrillary Aβ plaques is observed in regions where the accumulation of Aβ plaques begins in early disease stages. The co-localization of microglia and Aβ plaques has been previously studied by Boon et al., in which the direct co-localization of clustered microglia in classic-cored plaques in AD was demonstrated via immunofluorescence multi-labeling staining [59]. Similarly, via detailed CLSM, we observed that Aβ plaques co-localize directly with reactive amoeboid microglia in limbic and cortical regions [Fig. 5.].

Previous studies likewise reported that Iba1-positive microglia were highly present in control cases and represented mainly homeostatic microglia, and when double-labeling IHC was performed, mainly reactive swollen amoeboid Iba1-positive microglia were CD68-positive [85]. In addition, previous studies have described the appearance of Iba1-positive microglia in the healthy aging brain as unchanged [30, 32] or even more prevalent than in DLB or AD [31, 63, 86]. However, the significance of the increase in total microglial load with age in the CNS is still unclear [87]. Presumably, this is independent of the presence of pathology as it did not associate with pathological load. Therefore, a neuroprotective role, rather than a role in promoting disease progression, of Iba1-positive microglia could be hypothesized.

Conflicting results on activated CD68-positive or HLA-DR-positive microglia in DLB phenotypes have been reported previously, in which some studies found an increase in the amygdala, hippocampus, transentorhinal cortex and TC compared to controls [26, 27, 29, 30], while others did not report an increase in the hippocampus or neocortex [31, 32]. Besides, detailed transcriptomic analysis of post-mortem brain tissue in DLB failed to show microglial activation [34, 88]. We only observed a higher reactive microglial load in the CA2 in pure DLB cases compared to controls in our cohort. However, it is important to note that only one study distinguished pure DLB from mixed DLB+AD cases, reporting a higher load in mixed DLB than in pure DLB cases [29]. We found a similar pattern in our cohort, where mixed DLB+AD cases had a higher reactive microglial load than pure DLB cases in the amygdala and PHG. In addition, we confirmed the higher amoeboid and reactive microglial density in mixed DLB when compared to pure DLB cases. The contradicting results on microglial activity in DLB phenotypes are likely related to the fact that pure and mixed DLB cases were not separated in most cohorts. Moreover, results on microglial upregulation in DLB were based on studies with a small sample size, including only 5 DLB cases in each cohort [27, 29, 30], and different techniques for quantification were used between studies. Additionally,

we found strong associations between microglial activation and AD-pathology in mixed DLB+AD, pure AD and in pure DLB cases, whereas an association between microglial activation and α-syn pathology did not exist in pure DLB cases. In addition, overall microglial activation was the highest in regions with the highest burden of concomitant α-syn and p-tau pathology in our cohort, i.e. the CA2 and amygdala.

We confirmed significant upregulation of astrocytes in pure AD cases [89, 90]. Two studies in DLB reported an increased astrocytic response in the TC [33] and pulvinar [34] compared to controls, which we could not confirm in our results. However, α-syn accumulation in activated astrocytes has been reported in several studies [11, 37, 91, 92], suggesting a direct link between α-syn accumulation and activation of the innate immune system. Minor astrocytic differences between mixed and pure DLB cases in our cohort suggest astrocytic response to be mostly related to α-syn and not to AD co-pathology, and a region-specific association with α-syn in the amygdala suggests regional vulnerability [11]. Moreover, we did not find a high astroglial load in regions with a high burden of concomitant pathology. It is important to understand that despite being one of the most extensively used astrocytic markers, GFAP only labels the intermediate filament of the cytoskeleton of mature astrocytes, and is therefore not able to stain all astrocytes [93].

Confirming previous studies [94], we found a higher Aβ load in *APOEε4* carriers. In addition, microglial upregulation has previously been described in *APOEε4* carriers [57], which we confirmed in homozygous *APOEε4* carriers. In line with previous results [56], we demonstrated that pathogenic *GBA1* mutation carriers have less AD pathology and are most common in pure phenotypes of DLB. Subtypes of *HLA-DRB1*04* were previously described to protect against both PD and AD by improving immune clearance of NFTs [52]. However, we had a total of 11 cases with *HLA-DRB1*04* alleles in our cohort only, and were not able to reproduce these findings.

Overall, our study highlights the important role of microglial activation, specifically in mixed cases. Importantly, diverse clinical trials that either influence microglial activation in early disease stages, suppress pro-inflammatory responses of microglia or modulate microglial phenotypic changes to support anti-inflammatory capacities in AD are currently being investigated [95]. In addition, reliable biomarkers to measure AD pathology in CSF exist [96], supporting the opportunity to make an appropriate selection of mixed DLB cases for future clinical trials on immunomodulatory approaches.

Strengths of this study include being one of the first to investigate co-pathology and inflammation in a large number of brain regions in both mixed and pure DLB in a qualitative, semi-quantitative and quantitative manner.

Furthermore, multiple neuroinflammatory markers were evaluated, microglia response near plaques using confocal microscopy were studied, and the effects of common genotypes on neuropathology and inflammation were analyzed. However, although we studied a very well-defined cohort, the sample size and clinical information on disease severity were limited. Further, other pathologies, such as TDP-43, and molecular phenotypes of glial cells, to better understand their activation state, were not studied. Future research should focus on spatial transcriptomics to study the molecular phenotype of reactive microglia and astroglia surrounding (co-)pathology. Besides, the quantitative QuPath analyses detected the total %area of immunopositivity, and therefore detected all positive structures. An Artificial Intelligence based approach that would be able to distinguish the different morphological pathological and glial structures would be of great interest for future studies. Finally, studying the level of AD pathology and neuroinflammation via in-vivo biomarkers, e.g., in CSF or plasma, would enhance the investigation of a more comprehensive spectrum of disease stages.

Conclusion

In conclusion, we highlight that microglial activation in DLB is largely associated with AD co-pathology, whereas astrocytic response did not differ between DLB phenotypes. Most importantly, microglial activity was high in limbic regions, with prevalent AD pathology. We provide novel insights into the molecular neuropathology of DLB and the importance of microglial load, possibly underlying the more rapid disease progression in mixed DLB+AD. Glial biomarkers should be studied to provide insights into disease progression and, more importantly, support the selection of DLB phenotypes for future clinical trials on immunomodulatory approaches.

Abbreviations

α-syn	alpha-synuclein
Aβ	amyloid-beta
AD	Alzheimer disease
Amy	amygdala
CA	cornu ammonis
CD68	cluster of differentiation 68
CSF	cerebrospinal fluid
DG	dentate gyrus
DLB	dementia with Lewy bodies
EntC	entorhinal cortex
FusG	fusiform gyrus
GFAP	glial fibrillary acidic protein
GTM	medial temporal gyrus
HipMid	medial hippocampus
HLA-DR	human leukocyte antigen – DR isotype
Iba1	ionized calcium-binding adapter molecule 1
LBs	Lewy bodies
LNs	Lewy neurites
ParaSub	parasubiculum
PD	Parkinson's disease
PHG	parahippocampal gyrus
p-syn	phosphorylated alpha-synuclein
p-tau	phosphorylated tau
RBD	REM sleep behavior disorders
REM	rapid eye movement
ROI	region of interest
Sub	subiculum
TC	temporal cortex

Supplementary Information

The online version contains supplementary material available at https://doi.org/10.1186/s40478-024-01786-z.

Supplementary Material 1

Data availability
Supporting data include supplementary tables, supplementary figures, and supplementary material. Accessibility to raw outcome measures will be made available on reasonable request.

Declarations

Ethical approval and consent to participate
All donors signed an informed consent for brain donation and the use of material and clinical information for research purposes. The procedures for brain tissue collection of NBB and NABCA have been approved by the Medical Ethical Committee of Amsterdam UMC, Vrije Universiteit Amsterdam.

Consent for publication
Approved by all authors.

Competing interests
The authors declare that they have no competing interests for this study. WvdB was financially supported by grants from Dutch Research council (ZonMW 70-73305-98-106; 70-73305-98-102; 40-46000-98-101), Alzheimer association (AARF-18-566459), MJ Fox foundation (17253), Parkinson Association (2020-G01), Health Holland and Stichting Woelse Waard. WvdB performed contract research for Roche Tissue Diagnostics, Discoveric Bio and Genentech, and received research consumables from Hoffmann-La Roche and Prothena.

Author details
[1]Department of Anatomy and Neurosciences, Section Clinical Neuroanatomy and Biobanking and Life Sciences O|2 building 13e55, Amsterdam UMC location Vrije Universiteit Amsterdam, De Boelelaan 1118, Amsterdam 1081 HV, The Netherlands

[2]Neurodegeneration, Amsterdam Neuroscience, Amsterdam, The Netherlands

[3]Department of Epidemiology and Biostatistics, Amsterdam UMC location Vrije Universiteit Amsterdam, De Boelelaan 1117, Amsterdam, The Netherlands

[4]Department of Neurology, Leiden University Medical Center, Albinusdreef 2, Leiden 2333 ZA, The Netherlands

[5]Department of Neurology, Oslo University Hospital, Oslo, Norway

[6]Department of Neurology, Amsterdam UMC location Vrije Universiteit Amsterdam, Amsterdam, De Boelelaan 1117, The Netherlands

[7]Alzheimer Center, Department of Neurology, Amsterdam UMC, Vrije Universiteit Amsterdam, Amsterdam Neuroscience, Amsterdam, The Netherlands

[8]Department of Pathology, Amsterdam UMC location Vrije Universiteit Amsterdam, De Boelelaan 1117, Amsterdam, The Netherlands

References

1. Cunningham EL, McGuinness B, Herron B, Passmore AP (2015) Dementia. Ulster Med J 84(2):79–87
2. Lane CA, Hardy J, Schott JM (2018) Alzheimer's disease. Eur J Neurol 25(1):59–70. https://doi.org/10.1111/ene.13439
3. McKeith IG, Boeve BF, Dickson DW, Halliday G, Taylor JP, Weintraub D, Kosaka K (2017) Diagnosis and management of dementia with Lewy bodies: fourth consensus report of the DLB Consortium. Neurology 89(1):88–100. https://doi.org/10.1212/wnl.0000000000004058
4. Walker L, McAleese KE, Thomas AJ, Johnson M, Martin-Ruiz C, Parker C, Attems J (2015) Neuropathologically mixed Alzheimer's and Lewy body disease: burden of pathological protein aggregates differs between clinical phenotypes. Acta Neuropathol 129(5):729–748. https://doi.org/10.1007/s00401-015-1406-3
5. Geut H, Vergouw LJM, Galis Y, Ingrassia A, de Jong FJ, Quadri M, van de Berg WDJ (2019) Neuropathological and genetic characteristics of a post-mortem series of cases with dementia with Lewy bodies clinically suspected of Creutzfeldt-Jakob's disease. Parkinsonism Relat Disord 63:162–168. https://doi.org/10.1016/j.parkreldis.2019.02.011
6. Braak H, Alafuzoff I, Arzberger T, Kretzschmar H, Del Tredici K (2006) Staging of Alzheimer disease-associated neurofibrillary pathology using paraffin sections and immunocytochemistry. Acta Neuropathol 112(4):389–404. https://doi.org/10.1007/s00401-006-0127-z
7. Thal DR, Rüb U, Orantes M, Braak H (2002) Phases of a beta-deposition in the human brain and its relevance for the development of AD. Neurology 58(12):1791–1800. https://doi.org/10.1212/wnl.58.12.1791
8. Jellinger KA, Wenning GK, Seppi K (2007) Predictors of survival in dementia with lewy bodies and Parkinson dementia. Neurodegener Dis 4(6):428–430. https://doi.org/10.1159/000107703
9. Halliday GM, Holton JL, Revesz T, Dickson DW (2011) Neuropathology underlying clinical variability in patients with synucleinopathies. Acta Neuropathol 122(2):187–204. https://doi.org/10.1007/s00401-011-0852-9
10. Irwin DJ, Hurtig HI (2018) The contribution of tau, amyloid-Beta and alpha-Synuclein Pathology to Dementia in Lewy Body Disorders. J Alzheimers Dis Parkinsonism 8(4). https://doi.org/10.4172/2161-0460.1000444
11. Sorrentino ZA, Giasson BI, Chakrabarty P (2019) α-Synuclein and astrocytes: tracing the pathways from homeostasis to neurodegeneration in Lewy body disease. Acta Neuropathol 138(1):1–21. https://doi.org/10.1007/s00401-019-01977-2
12. Nelson PT, Abner EL, Patel E, Anderson S, Wilcock DM, Kryscio RJ, Cykowski MD (2018) The Amygdala as a locus of pathologic misfolding in neurodegenerative diseases. J Neuropathol Exp Neurol 77(1):2–20. https://doi.org/10.1093/jnen/nlx099
13. Peng C, Trojanowski JQ, Lee VM (2020) Protein transmission in neurodegenerative disease. Nat Rev Neurol 16(4):199–212. https://doi.org/10.1038/s41582-020-0333-7
14. Vasili E, Dominguez-Meijide A, Outeiro TF (2019) Spreading of α-Synuclein and tau: a systematic comparison of the mechanisms involved. Front Mol Neurosci 12:107. https://doi.org/10.3389/fnmol.2019.00107
15. Moussaud S, Jones DR, Moussaud-Lamodière EL, Delenclos M, Ross OA, McLean PJ (2014) Alpha-synuclein and tau:

16. teammates in neurodegeneration? Mol Neurodegen 9:43. https://doi.org/10.1186/1750-1326-9-43
16. Marsh SE, Blurton-Jones M (2012) Examining the mechanisms that link β-amyloid and α-synuclein pathologies. Alzheimers Res Ther 4(2):11. https://doi.org/10.1186/alzrt109
17. Outeiro TF, Koss DJ, Erskine D, Walker L, Kurzawa-Akanbi M, Burn D, McKeith I (2019) Dementia with Lewy bodies: an update and outlook. Mol Neurodegener 14(1):5. https://doi.org/10.1186/s13024-019-0306-8
18. Lemstra AW, de Beer MH, Teunissen CE, Schreuder C, Scheltens P, van der Flier WM, Sikkes SA (2017) Concomitant AD pathology affects clinical manifestation and survival in dementia with Lewy bodies. J Neurol Neurosurg Psychiatry 88(2):113–118. https://doi.org/10.1136/jnnp-2016-313775
19. Ferman TJ, Aoki N, Boeve BF, Aakre JA, Kantarci K, Graff-Radford J, Dickson DW (2020) Subtypes of dementia with Lewy bodies are associated with alpha-synuclein and tau distribution. Neurology 95(2):e155–e165. https://doi.org/10.1212/WNL.0000000000009763
20. Ferreira D, Przybelski SA, Lesnick TG, Lemstra AW, Londos E, Blanc F, Kantarci K (2020) β-Amyloid and tau biomarkers and clinical phenotype in dementia with Lewy bodies. Neurology 95(24):e3257–e3268. https://doi.org/10.1212/wnl.0000000000010943
21. Fixemer S, Ameli C, Hammer G, Salamanca L, Uriarte Huarte O, Schwartz C, Bouvier DS (2022) Microglia phenotypes are associated with subregional patterns of concomitant tau, amyloid-β and α-synuclein pathologies in the hippocampus of patients with Alzheimer's disease and dementia with Lewy bodies. Acta Neuropathol Commun 10(1):36. https://doi.org/10.1186/s40478-022-01342-7
22. Baik SH, Kang S, Son SM, Mook-Jung I (2016) Microglia contributes to plaque growth by cell death due to uptake of amyloid β in the brain of Alzheimer's disease mouse model. Glia 64(12):2274–2290. https://doi.org/10.1002/glia.23074
23. Guzman-Martinez L, Maccioni RB, Andrade V, Navarrete LP, Pastor MG, Ramos-Escobar N (2019) Neuroinflammation as a common feature of neurodegenerative disorders. Front Pharmacol 10:1008. https://doi.org/10.3389/fphar.2019.01008
24. Fellner L, Irschick R, Schanda K, Reindl M, Klimaschewski L, Poewe W, Stefanova N (2013) Toll-like receptor 4 is required for α-synuclein dependent activation of microglia and astroglia. Glia 61(3):349–360. https://doi.org/10.1002/glia.22437
25. Heneka MT, Carson MJ, Khoury E, Landreth J, Brosseron GE, Feinstein F, Kummer DL, M. P (2015) Neuroinflammation in Alzheimer's disease. Lancet Neurol 14(4):388–405. https://doi.org/10.1016/s1474-4422(15)70016-5
26. Kouli A, Camacho M, Allinson K, Williams-Gray CH (2020) Neuroinflammation and protein pathology in Parkinson's disease dementia. Acta Neuropathol Commun 8(1):211. https://doi.org/10.1186/s40478-020-01083-5
27. Imamura K, Hishikawa N, Sawada M, Nagatsu T, Yoshida M, Hashizume Y (2003) Distribution of major histocompatibility complex class II-positive microglia and cytokine profile of Parkinson's disease brains. Acta Neuropathol 106(6):518–526. https://doi.org/10.1007/s00401-003-0766-2
28. Doorn KJ, Moors T, Drukarch B, van de Berg W, Lucassen PJ, van Dam AM (2014) Microglial phenotypes and toll-like receptor 2 in the substantia nigra and hippocampus of incidental Lewy body disease cases and Parkinson's disease patients. Acta Neuropathol Commun 2:90. https://doi.org/10.1186/s40478-014-0090-1
29. Mackenzie IR (2000) Activated microglia in dementia with Lewy bodies. Neurology 55(1):132–134. https://doi.org/10.1212/wnl.55.1.132
30. Streit WJ, Xue QS (2016) Microglia in dementia with Lewy bodies. Brain Behav Immun 55:191–201. https://doi.org/10.1016/j.bbi.2015.10.012
31. Bachstetter AD, Van Eldik LJ, Schmitt FA, Neltner JH, Ighodaro ET, Webster SJ, Nelson PT (2015) Disease-related microglia heterogeneity in the hippocampus of Alzheimer's disease, dementia with Lewy bodies, and hippocampal sclerosis of aging. Acta Neuropathol Commun 3:32. https://doi.org/10.1186/s40478-015-0209-z
32. Amin J, Holmes C, Dorey RB, Tommasino E, Casal YR, Williams DM, Boche D (2020) Neuroinflammation in dementia with Lewy bodies: a human post-mortem study. Transl Psychiatry 10(1):267. https://doi.org/10.1038/s41398-020-00954-8
33. Tu H, Zhang ZW, Qiu L, Lin Y, Jiang M, Chia SY, Zeng L (2022) Increased expression of pathological markers in Parkinson's disease dementia post-mortem brains compared to dementia with Lewy bodies. BMC Neurosci 23(1):3. https://doi.org/10.1186/s12868-021-00687-4
34. Erskine D, Ding J, Thomas AJ, Kaganovich A, Khundakar AA, Hanson PS, Morris CM (2018) Molecular changes in the absence of severe pathology in the

34. pulvinar in dementia with Lewy bodies. Mov Disord 33(6):982–991. https://doi.org/10.1002/mds.27333

35. Amin J, Erskine D, Donaghy PC, Surendranathan A, Swann P, Kunicki AP, Thomas AJ (2022) Inflammation in dementia with Lewy bodies. Neurobiol Dis 168:105698. https://doi.org/10.1016/j.nbd.2022.105698

36. Eikelenboom P, Rozemuller AJ, Hoozemans JJ, Veerhuis R, van Gool WA (2000) Neuroinflammation and Alzheimer disease: clinical and therapeutic implications. Alzheimer Dis Assoc Disord 14(Suppl 1):S54–61. https://doi.org/10.1097/00002093-200000001-00009

37. Surendranathan A, Rowe JB, O'Brien JT (2015) Neuroinflammation in Lewy body dementia. Parkinsonism Relat Disord 21(12):1398–1406. https://doi.org/10.1016/j.parkreldis.2015.10.009

38. Ransohoff RM (2016) How neuroinflammation contributes to neurodegeneration. Science 353(6301):777–783. https://doi.org/10.1126/science.aag2590

39. Morenas-Rodríguez E, Alcolea D, Suárez-Calvet M, Muñoz-Llahuna L, Vilaplana E, Sala I, Lleó A (2019) Different pattern of CSF glial markers between dementia with Lewy bodies and Alzheimer's disease. Sci Rep 9(1):7803. https://doi.org/10.1038/s41598-019-44173-8

40. Llorens F, Thüne K, Tahir W, Kanata E, Diaz-Lucena D, Xanthopoulos K, Zerr I (2017) YKL-40 in the brain and cerebrospinal fluid of neurodegenerative dementias. Mol Neurodegener 12(1):83. https://doi.org/10.1186/s13024-017-0226-4

41. Rozemuller AJ, Eikelenboom P, Theeuwes JW, Steur J, E. N., de Vos RA (2000) Activated microglial cells and complement factors are unrelated to cortical Lewy bodies. Acta Neuropathol 100(6):701–708. https://doi.org/10.1007/s004010000225

42. Walker DG, Lue LF, Tang TM, Adler CH, Caviness JN, Sabbagh MN, Beach TG (2017) Changes in CD200 and intercellular adhesion molecule-1 (ICAM-1) levels in brains of Lewy body disorder cases are associated with amounts of Alzheimer's pathology not α-synuclein pathology. Neurobiol Aging 54:175–186. https://doi.org/10.1016/j.neurobiolaging.2017.03.007

43. Altay MF, Liu AKL, Holton JL, Parkkinen L, Lashuel HA (2022) Prominent astrocytic alpha-synuclein pathology with unique post-translational modification signatures unveiled across Lewy body disorders. Acta Neuropathol Commun 10(1):163. https://doi.org/10.1186/s40478-022-01468-8

44. Fathy YY, Jonker AJ, Oudejans E, de Jong FJJ, van Dam AW, Rozemuller AJM, van de Berg WDJ (2019) Differential insular cortex subregional vulnerability to α-synuclein pathology in Parkinson's disease and dementia with Lewy bodies. Neuropathol Appl Neurobiol 45(3):262–277. https://doi.org/10.1111/nan.12501

45. Myers AJ, Brahimi A, Jenkins IJ, Koob AO (2023) The synucleins and the astrocyte. Biology (Basel) 12(2). https://doi.org/10.3390/biology12020155

46. Chauveau F, Boutin H, Van Camp N, Dollé F, Tavitian B (2008) Nuclear imaging of neuroinflammation: a comprehensive review of [11 C]PK11195 challengers. Eur J Nucl Med Mol Imaging 35(12):2304–2319. https://doi.org/10.1007/s00259-008-0908-9

47. Iannaccone S, Cerami C, Alessio M, Garibotto V, Panzacchi A, Olivieri S, Perani D (2013) In vivo microglia activation in very early dementia with Lewy bodies, comparison with Parkinson's disease. Parkinsonism Relat Disord 19(1):47–52. https://doi.org/10.1016/j.parkreldis.2012.07.002

48. Surendranathan A, Su L, Mak E, Passamonti L, Hong YT, Arnold R, O'Brien JT (2018) Early microglial activation and peripheral inflammation in dementia with Lewy bodies. Brain 141(12):3415–3427. https://doi.org/10.1093/brain/awy265

49. Cagnin A, Brooks DJ, Kennedy AM, Gunn RN, Myers R, Turkheimer FE, Banati RB (2001) In-vivo measurement of activated microglia in dementia. Lancet 358(9280):461–467. https://doi.org/10.1016/s0140-6736(01)05625-2

50. Cerami C, Iaccarino L, Perani D (2017) Molecular Imaging of Neuroinflammation in neurodegenerative dementias: the role of in vivo PET imaging. Int J Mol Sci 18(5). https://doi.org/10.3390/ijms18050993

51. Le Guen Y, Luo G, Ambati A, Damotte V, Jansen I, Yu E, Mignot E (2023) Multiancestry analysis of the HLA locus in Alzheimer's and Parkinson's diseases uncovers a shared adaptive immune response mediated by HLA-DRB1*04 subtypes. Proc Natl Acad Sci U S A 120(36):e2302720120. https://doi.org/10.1073/pnas.2302720120

52. Guen YL, Luo G, Ambati A, Damotte V, Jansen I, Yu E, Mignot E (2021) Protective association of HLA-DRB1*04 subtypes in neurodegenerative diseases implicates acetylated Tau PHF6 sequences. *medRxiv*, 2021.2012.2026.21268354. https://doi.org/10.1101/2021.12.26.21268354

53. Yu E, Ambati A, Andersen MS, Krohn L, Estiar MA, Saini P, Gan-Or Z (2021) Fine mapping of the HLA locus in Parkinson's disease in europeans. NPJ Parkinsons Dis 7(1):84. https://doi.org/10.1038/s41531-021-00231-5

54. Robinson JL, Lee EB, Xie SX, Rennert L, Suh E, Bredenberg C, Trojanowski JQ (2018) Neurodegenerative disease concomitant proteinopathies are prevalent, age-related and APOE4-associated. Brain 141(7):2181–2193. https://doi.org/10.1093/brain/awy146

55. Minett T, Classey J, Matthews FE, Fahrenhold M, Taga M, Brayne C, Mrc C (2016) Microglial immunophenotype in dementia with Alzheimer's pathology. J Neuroinflamm 13(1):135. https://doi.org/10.1186/s12974-016-0601-z

56. Clark LN, Kartsaklis LA, Gilbert W, Dorado R, Ross B, Kisselev BM, Marder S, K (2009) Association of glucocerebrosidase mutations with dementia with lewy bodies. Arch Neurol 66(5):578–583. https://doi.org/10.1001/archneurol.2009.54

57. Minett T, Classey J, Matthews FE, Fahrenhold M, Taga M, Brayne C, Boche D (2016) Microglial immunophenotype in dementia with Alzheimer's pathology. J Neuroinflammation 13(1):135. https://doi.org/10.1186/s12974-016-0601-z

58. Montine TJ, Phelps CH, Beach TG, Bigio EH, Cairns NJ, Dickson DW, Hyman BT (2012) National Institute on Aging-Alzheimer's Association guidelines for the neuropathologic assessment of Alzheimer's disease: a practical approach. Acta Neuropathol 123(1):1–11. https://doi.org/10.1007/s00401-011-0910-3

59. Boon BDC, Hoozemans JJM, Lopuhaä B, Eigenhuis KN, Scheltens P, Kamphorst W, Bouwman FH (2018) Neuroinflammation is increased in the parietal cortex of atypical Alzheimer's disease. J Neuroinflammation 15(1):170. https://doi.org/10.1186/s12974-018-1180-y

60. Bankhead P, Loughrey MB, Fernandez JA, Dombrowski Y, McArt DG, Dunne PD, Hamilton PW (2017) QuPath: open source software for digital pathology image analysis. Sci Rep 7(1):16878. https://doi.org/10.1038/s41598-017-17204-5

61. Schumann CM, Amaral DG (2005) Stereological estimation of the number of neurons in the human amygdaloid complex. J Comp Neurol 491(4):320–329. https://doi.org/10.1002/cne.20704

62. Duvernoy H (2005) Anatomy. In The Human Hippocampus: Functional Anatomy, Vascularization and Serial Sections with MRI (pp. 39–72). Berlin, Heidelberg: *Springer Berlin Heidelberg*

63. Hopperton KE, Mohammad D, Trépanier MO, Giuliano V, Bazinet RP (2018) Markers of microglia in post-mortem brain samples from patients with Alzheimer's disease: a systematic review. Mol Psychiatry 23(2):177–198. https://doi.org/10.1038/mp.2017.246

64. Paolicelli RC, Sierra A, Stevens B, Tremblay ME, Aguzzi A, Ajami B, Wyss-Coray T (2022) Microglia states and nomenclature: a field at its crossroads. Neuron 110(21):3458–3483. https://doi.org/10.1016/j.neuron.2022.10.020

65. Reddaway J, Richardson PE, Bevan RJ, Stoneman J, Palombo M (2023) Microglial morphometric analysis: so many options, so little consistency. Front Neuroinform 17:1211188. https://doi.org/10.3389/fninf.2023.1211188

66. Sofroniew MV, Vinters HV (2010) Astrocytes: biology and pathology. Acta Neuropathol 119(1):7–35. https://doi.org/10.1007/s00401-009-0619-8

67. Zhou B, Zuo YX, Jiang RT (2019) Astrocyte morphology: diversity, plasticity, and role in neurological diseases. CNS Neurosci Ther 25(6):665–673. https://doi.org/10.1111/cns.13123

68. Tunold JA, Tan MMX, Koga S, Geut H, Rozemuller AJM, Valentino R, Pihlstrøm L (2023) Lysosomal polygenic risk is associated with the severity of neuropathology in Lewy body disease. Brain 146(10):4077–4087. https://doi.org/10.1093/brain/awad183

69. Moors TE, Paciotti S, Ingrassia A, Quadri M, Breedveld G, Tasegian A, van de Berg WDJ (2019) Characterization of Brain lysosomal activities in GBA-Related and sporadic Parkinson's Disease and Dementia with Lewy Bodies. Mol Neurobiol 56(2):1344–1355. https://doi.org/10.1007/s12035-018-1090-0

70. Jia X, Han B, Onengut-Gumuscu S, Chen WM, Concannon PJ, Rich SS, de Bakker PI (2013) Imputing amino acid polymorphisms in human leukocyte antigens. PLoS ONE 8(6):e64683. https://doi.org/10.1371/journal.pone.0064683

71. Hochberg Y, Benjamini Y (1990) More powerful procedures for multiple significance testing. Stat Med 9(7):811–818. https://doi.org/10.1002/sim.4780090710

72. Attems J, Jellinger KA (2004) Only cerebral capillary amyloid angiopathy correlates with Alzheimer pathology–a pilot study. Acta Neuropathol 107(2):83–90. https://doi.org/10.1007/s00401-003-0796-9

73. Montine TJ, Phelps CH, Beach TG, Bigio EH, Cairns NJ, Dickson DW, Alzheimer's A (2012) National Institute on Aging-Alzheimer's Association guidelines for the neuropathologic assessment of Alzheimer's disease: a practical approach. Acta Neuropathol 123(1):1–11. https://doi.org/10.1007/s00401-011-0910-3

74. Hendrickx DAE, van Eden CG, Schuurman KG, Hamann J, Huitinga I (2017) Staining of HLA-DR, Iba1 and CD68 in human microglia reveals partially

overlapping expression depending on cellular morphology and pathology. J Neuroimmunol 309:12–22. https://doi.org/10.1016/j.neuroim.2017.04.007

75. Kamphuis W, Middeldorp J, Kooijman L, Sluijs JA, Kooi EJ, Moeton M, Hol EM (2014) Glial fibrillary acidic protein isoform expression in plaque related astrogliosis in Alzheimer's disease. Neurobiol Aging 35(3):492–510. https://doi.org/10.1016/j.neurobiolaging.2013.09.035

76. Thal DR, Rüb U, Schultz C, Sassin I, Ghebremedhin E, Del Tredici K, Braak H (2000) Sequence of Abeta-protein deposition in the human medial temporal lobe. J Neuropathol Exp Neurol 59(8):733–748. https://doi.org/10.1093/jnen/59.8.733

77. Walker LC (2020) Aβ plaques. Free Neuropathol. 110.17879/freeneuropathology-2020-3025

78. Coughlin D, Xie SX, Liang M, Williams A, Peterson C, Weintraub D, Irwin DJ (2019) Cognitive and pathological influences of Tau Pathology in Lewy Body Disorders. Ann Neurol 85(2):259–271. https://doi.org/10.1002/ana.25392

79. Ferman TJ, Aoki N, Crook JE, Murray ME, Graff-Radford NR, van Gerpen JA, Dickson DW (2018) The limbic and neocortical contribution of alpha-synuclein, tau, and amyloid beta to disease duration in dementia with Lewy bodies. Alzheimers Dement 14(3):330–339. https://doi.org/10.1016/j.jalz.2017.09.014

80. Toledo JB, Gopal P, Raible K, Irwin DJ, Brettschneider J, Sedor S, Trojanowski JQ (2016) Pathological alpha-synuclein distribution in subjects with coincident Alzheimer's and Lewy body pathology. Acta Neuropathol 131(3):393–409. https://doi.org/10.1007/s00401-015-1526-9

81. Braak H, Del Tredici K, Rüb U, de Vos RA, Steur J, E. N., Braak E (2003) Staging of brain pathology related to sporadic Parkinson's disease. Neurobiol Aging 24(2):197–211. https://doi.org/10.1016/s0197-4580(02)00065-9

82. Armstrong RA, Cairns NJ, Lantos PL (2000) Beta-amyloid deposition in the temporal lobe of patients with dementia with Lewy bodies: comparison with non-demented cases and Alzheimer's disease. Dement Geriatr Cogn Disord 11(4):187–192. https://doi.org/10.1159/000017235

83. Lee CY, Landreth GE (2010) The role of microglia in amyloid clearance from the AD brain. J Neural Transm (Vienna) 117(8):949–960. https://doi.org/10.1007/s00702-010-0433-4

84. Merlo S, Spampinato SF, Caruso GI, Sortino MA (2020) The ambiguous role of Microglia in Aβ toxicity: chances for therapeutic intervention. Curr Neuropharmacol 18(5):446–455. https://doi.org/10.2174/1570159x18666200131105418

85. Waller R, Baxter L, Fillingham DJ, Coelho S, Pozo JM, Mozumder M, Highley JR (2019) Iba-1-/CD68+ microglia are a prominent feature of age-associated deep subcortical white matter lesions. PLoS ONE 14(1):e0210888. https://doi.org/10.1371/journal.pone.0210888

86. Paasila PJ, Davies DS, Kril JJ, Goldsbury C, Sutherland GT (2019) The relationship between the morphological subtypes of microglia and Alzheimer's disease neuropathology. Brain Pathol 29(6):726–740. https://doi.org/10.1111/bpa.12717

87. Wong WT (2013) Microglial aging in the healthy CNS: phenotypes, drivers, and rejuvenation. Front Cell Neurosci 7:22. https://doi.org/10.3389/fncel.2013.00022

88. Rajkumar AP, Bidkhori G, Shoaie S, Clarke E, Morrin H, Hye A, Aarsland D (2020) Postmortem Cortical Transcriptomics of Lewy Body Dementia Reveal Mitochondrial Dysfunction and lack of Neuroinflammation. Am J Geriatr Psychiatry 28(1):75–86. https://doi.org/10.1016/j.jagp.2019.06.007

89. Price BR, Johnson LA, Norris CM (2021) Reactive astrocytes: the nexus of pathological and clinical hallmarks of Alzheimer's disease. Ageing Res Rev 68:101335. https://doi.org/10.1016/j.arr.2021.101335

90. Bras J, Guerreiro R, Darwent L, Parkkinen L, Ansorge O, Escott-Price V, Hardy J (2014) Genetic analysis implicates APOE, SNCA and suggests lysosomal dysfunction in the etiology of dementia with Lewy bodies. Hum Mol Genet 23(23):6139–6146. https://doi.org/10.1093/hmg/ddu334

91. Klegeris A, Pelech S, Giasson BI, Maguire J, Zhang H, McGeer EG, McGeer PL (2008) Alpha-synuclein activates stress signaling protein kinases in THP-1 cells and microglia. Neurobiol Aging 29(5):739–752. https://doi.org/10.1016/j.neurobiolaging.2006.11.013

92. Croisier E, Moran LB, Dexter DT, Pearce RK, Graeber MB (2005) Microglial inflammation in the parkinsonian substantia nigra: relationship to alpha-synuclein deposition. J Neuroinflammation 2:14. https://doi.org/10.1186/1742-2094-2-14

93. Preston AN, Cervasio DA, Laughlin ST (2019) Visualizing the brain's astrocytes. Methods Enzymol 622:129–151. https://doi.org/10.1016/bs.mie.2019.02.006

94. Raulin AC, Doss SV, Trottier ZA, Ikezu TC, Bu G, Liu CC (2022) ApoE in Alzheimer's disease: pathophysiology and therapeutic strategies. Mol Neurodegener 17(1):72. https://doi.org/10.1186/s13024-022-00574-4

95. Leng F, Edison P (2021) Neuroinflammation and microglial activation in Alzheimer disease: where do we go from here? Nat Rev Neurol 17(3):157–172. https://doi.org/10.1038/s41582-020-00435-y

96. van Steenoven I, Aarsland D, Weintraub D, Londos E, Blanc F, van der Flier WM, Lemstra AW (2016) Cerebrospinal fluid Alzheimer's disease biomarkers across the Spectrum of Lewy Body diseases: results from a large Multicenter Cohort. J Alzheimers Dis 54(1):287–295. https://doi.org/10.3233/jad-160322

Publisher's Note

N.a. = not available. N.s. = no significant difference between groups. A = controls vs. pure AD; B = controls vs. pure DLB; C = controls vs. mixed DLB + AD; D = pure AD vs. pure DLB; E = pure AD vs. mixed DLB + AD; F = pure DLB vs. mixed DLB + AD. CAA = cerebral amyloid angiopathy; CERAD = Consortium to Establish a Registry for Alzheimer Disease; *APOEε* = apolipoprotein E; *HLA-DRB1*04 = human leukocyte antigen DRB1*04 subtypes; *GBA1* = glucocerebrosidase gene 1. Groups were compared using a one-way ANOVA with post-hoc t-tests for continuous and a Fisher's exact test with post-hoc pairwise comparisons for categorical variables. Post-hoc tests were performed if overall test was significant Heatmap of standardized regression coefficients between microglial or astrocytic load and α-syn, Aβ and p-tau pathological load over all groups. Positive standardized regression coefficients are depicted in red, while negative standardized regression coefficients are denoted in blue in the heatmap. Significance is demonstrated in bold as * $p < 0.05$, ** $p < 0.01$, and *** $p < 0.001$